

Fully biobased triblock copolymers generated using an unconventional oscillatory plug flow reactor

Peer-reviewed author version

DEN HAESE, Milan; Gemoets, Hannes P. L.; Van Aken, Koen & PITET, Louis (2022) Fully biobased triblock copolymers generated using an unconventional oscillatory plug flow reactor. In: Polymer chemistry, 13 (30) , p. 4406 -4415.

DOI: 10.1039/d2py00600f

Handle: <http://hdl.handle.net/1942/37891>

# Fully Biobased Triblock Copolymers Generated Using an Unconventional Oscillatory Plug Flow Reactor

Milan Den Haese<sup>1</sup>, Hannes P. L. Gemoets<sup>2</sup>, Koen Van Aken<sup>2</sup>, Louis M. Pitet<sup>1\*</sup>

<sup>1</sup>*Advanced Functional Polymers Laboratory, Institute for Materials Research (IMO), Hasselt University, Martelarenlaan 42, 3500 Hasselt, Belgium.*

<sup>2</sup>*Creaflow B.V., Industrielaan 12, 9800 Deinze, Belgium*

## ABSTRACT

Producing polymers in continuous flow offers significant advantages in terms of efficiency, scalability, and safety. Using conventional tubular flow reactors to synthesize polymers comes with some challenges, especially related to maintaining narrow residence time distributions (RTD) when operating with viscous fluids. Laminar flow is typically observed in tubes with restricted dimensions, and significant wall effects result in the broadening of the molar mass distributions. We envisioned that such a limitation can be overcome by the use of an oscillatory flow reactor (OFR). This work describes the use of a novel plate-type OFR to improve continuous-flow polymerization reactions for the first time. The reactor plate is equipped with millimeter-scale cubic pillars, and when combined with a superimposed oscillatory flow regime, promotes turbulent flow to circumvent detrimental wall effects during polymerizations. Additionally, the pulsatile flow intensifies mixing, and careful tuning of the pulsation amplitude and frequency lead to improved (i.e., narrowed) residence time distributions, a crucial parameter when synthesizing complex block polymer scaffolds in continuous flow. This innovative principle of implementing OFRs for improved continuous polymerization reaction is demonstrated with the benchmark ring-opening polymerization of lactide, a well-known renewable monomer. Thorough characterization using the reactor system reveals the relationships between process conditions and molecular attributes, including target molar mass and dispersity ( $\bar{M}_w/\bar{M}_n$ ). Further, the OFR enabled the streamlined

1 preparation of a series of block polymers with variable composition and low dispersity in a single  
2 experiment by judiciously adjusting the independent inlet feed rates. Finally, the OFR system  
3 allows for simple scaling without affecting the critical process parameters. As a result, a multi-  
4 gram synthetic protocol was achieved employing a biobased hydroxyl telechelic poly( $\beta$ -  
5 farnesene) macroinitiator in the ring-opening polymerization of lactide to generate fully renewable  
6 ABA-type triblock copolymers.

## 7 8 **INTRODUCTION**

9 Block polymers are macromolecules with segments of different repeating units that are covalently  
10 bound to each other.<sup>1</sup> Such segmented copolymers exhibit strongly composition dependent  
11 properties related to the adoption of various nanoscale morphologies, the formation of which is  
12 driven by the thermodynamic immiscibility between the constituent blocks.<sup>2, 3</sup> The properties can  
13 therefore be tuned by preparing products with different relative block lengths and different block  
14 sequences.<sup>4, 5</sup> However, each individual target composition typically requires a separate  
15 synthesis, which can be quite elaborate depending on the architecture.<sup>6-9</sup> This is nearly always  
16 carried out in batch reactions with each block made sequentially, which is especially necessary  
17 with mechanistically incommensurate monomers/repeating units.<sup>10-12</sup> Preparing even a limited  
18 series of block polymers with different compositions is tedious and resource intensive (e.g.,  
19 solvents, purification/precipitation). To mitigate this, preparing block polymers in continuous flow  
20 reactors has many appealing benefits, as outlined extensively in several recent reviews.<sup>13, 14</sup> In  
21 fact, preparation of block copolymers has been reported using various polymerization methods,  
22 using both a macroinitiator approach, sequential monomer addition, or coupling of preformed  
23 chains.<sup>15-23</sup> This has been demonstrated routinely with acrylates or lactones, typically using  
24 conventional tubular reactors or microfluidic devices. Flow polymerizations have received  
25 significant attention, with increasingly sophisticated adaptations being made recently to  
26 incorporate real-time feedback and machine learning in order to fully automate the process and

1 produce highly customizable polymer constructs.<sup>24-26</sup> Despite these gains, the conventional  
2 approach of using micrometer- or millimeter sized tubular reactors is still firmly the status quo.<sup>27</sup>  
3 <sup>28</sup> Such reactor geometries severely limit the scale on which materials can be produced. Full  
4 characterization of block polymers, especially for applications like thermoplastic elastomers,  
5 requires multi-gram synthetic protocols. Recently, a scalable oscillatory flow reactor (OFR) with a  
6 planar reaction compartment (15 mL internal capacity) has been used to successfully conduct  
7 organic small molecule transformations when processing challenging media (e.g., slurries,  
8 viscous solutions).<sup>29-32</sup> Polymerizations typically lead to increasing viscosities, which also  
9 challenges the integrity of mixing profiles. The novel OFR described in this work (*i.e.* HANU Flow  
10 Reactor, Creaflow B.V.) contains millimeter-sized cubic pillars that enhance turbulent flow, and  
11 thus promote intimate mixing. Furthermore, the unique oscillatory plug flow conditions enabled by  
12 a pulsator attached in-line to the reactor creates a continuous reaction pathway that does not  
13 compromise residence time distributions across a broad range of flow rates.<sup>33</sup> This allows a  
14 scalable production of materials (*i.e.*, grams per hour) in which the inlet/reactant delivery rates  
15 can be adjusted *in situ* to tailor the product makeup. This is an ideal setup for producing a library  
16 of block polymers with variable composition in a "single-pot", streamlined manner without the  
17 need for separate reactors and tedious product isolation protocols. Additionally, control over the  
18 polymerization, leading to low dispersities and accurate molar mass targeting, is not compromised  
19 by the viscous nature of the reaction medium. Here, we demonstrate the capabilities of the HANU  
20 flow reactor by conducting the organo-catalyzed ring-opening transesterification polymerization  
21 (ROTEP) of D,L-lactide (LA). Several lactones have been polymerized in a continuous-flow setup  
22 recently, but this has been limited to tubular or microfluidic devices.<sup>22, 34-37</sup> A range of molar  
23 masses ( $M_n$ ) have been targeted, highlighting the limitations and versatility, covering a broad  
24 spectrum of flow rates. Dispersity ( $\mathcal{D}$ ) of the resulting amorphous polylactide (PLA) was sensitive  
25 to the amplitude of the oscillation, but less dependent on the frequency. Finally, a series of ABA-  
26 type symmetric block polymers was prepared using optimized conditions in a single-experiment

by adjusting the inlet flow rates. We used a biobased hydroxyl-telechelic poly( $\beta$ -farnesene) as a macroinitiator in the ROP of LA monomer, producing a range of compositionally variable block polymers on multi-gram scale. Poly( $\beta$ -farnesene) is hydrophobic polymer derived from terpenes, a class of highly promising renewable monomers that have wide ranging properties.<sup>38-41</sup> Telechelic poly(farnesene) diol (PFD) has already been used in the context of hydrolysis resistant biobased polyurethane precursors.<sup>42</sup> Likewise, a related telechelic terpene derivative, poly(myrcene) has been shown to be effective as a midblock by polymerizing LA monomer, exhibiting the utility of such building blocks in generating triblock copolymers.<sup>43</sup> The resulting fully biobased thermoplastics described in this work exhibit a range of physical properties owing to the easily adjustable chemical composition, representing an ideal platform as potential biobased elastomers.<sup>44, 45</sup> Expanding the technological toolbox to provide convenient access to such a library of biobased block polymers is a highlight.

## RESULTS AND DISCUSSION

Our initial aim was to interrogate the continuous process conditions for polymerizations by implementing the oscillatory flow reactor (i.e., HANU flow reactor) and establish optimal settings for minimizing the residence time distribution (RTD) in reactions with progressively increasing viscosity (see supplementary information for a detailed description of the reactor; Figure S1).<sup>46</sup> The HANU flow reactor has a planar reaction chamber with 15 mL internal capacity. There is a series of regularly spaced stainless steel cube-shaped pillars situated throughout the reaction chamber. The pillars provide a split-and-recombine flow pattern and thus aid in uniform mixing. Further enhancement of the mixing profile is provided by a pulsator unit, which is positioned directly before the reactor inlet. This unit provides superimposed pulsation on the liquid flow. The amplitude and frequency of the pulsation can be independently tuned to optimize the product attributes, which in the case of polymerization is primarily reflected by the molar mass (i.e., conversion) and the molar mass distribution (i.e., dispersity –  $\bar{D}$ ).<sup>47</sup> The dependence of flow

profiles on pulsation conditions was initially analyzed qualitatively by visualizing the distribution of a dye as it travels through the reaction chamber. Initial experiments were conducted by adding an organic dye to acetone and then subsequently loading the colored solvent into the injector syringe. A plug volume of 0.5 mL was visually observed for its flow behavior (Figure 1). In the absence of pulsation (i.e., steady-state flow), a longitudinal spread of the tracer can be observed owing to the lateral velocity gradient present within the reactor channel leading to a distinct laminar flow profile with tailing observed on both sides of the process channel. In contrast, setting the pulsator to a low amplitude setting (5%, equal to 0.04 mL/stroke displacement) and low frequency (0.6 Hz) counteracted the observed tailing effect and led to a more compact, plug flow profile (i.e., narrow RTD) (Figure 1A, B) and is consistent with previously reported observations for small molecule synthesis.<sup>30</sup> In order to take a closer look at the effect of viscosity on the RTD, polyethylene glycol (PEG) with a number average molar mass ( $M_n$ ) of 1000 g/mol was dissolved in acetone to form a 0.8 M solution and subsequently colored using the same organic dye. The resulting polymer solution was significantly more viscous than the acetone solvent. Previous studies point toward the deleterious effect of increasing viscosity on mixing profiles, typically leading to increased RTD and thus higher dispersities.<sup>47, 48</sup> In this simple experiment in the OFR, improved plug-like flow behavior was visually observed when moderate frequencies (0.6–1.5 Hz) and low amplitudes ( $\leq 0.04$  mL/stroke) were employed (Figure 1C). On the other hand, when using higher pulsation amplitudes ( $> 0.08$  mL/stroke; 10% amplitude setting) this effect was no longer observed, as intensified mixing promotes a smearing effect because of the increased energy dissipation present. Additionally, it is worth noting that steady-state flow of the PEG solution leads to a longitudinal spread that is significantly more pronounced than that of the pure solvent case, indicating that the lateral velocity gradient increases with higher viscosity fluids due to the more significant wall effects (Figure 1C).

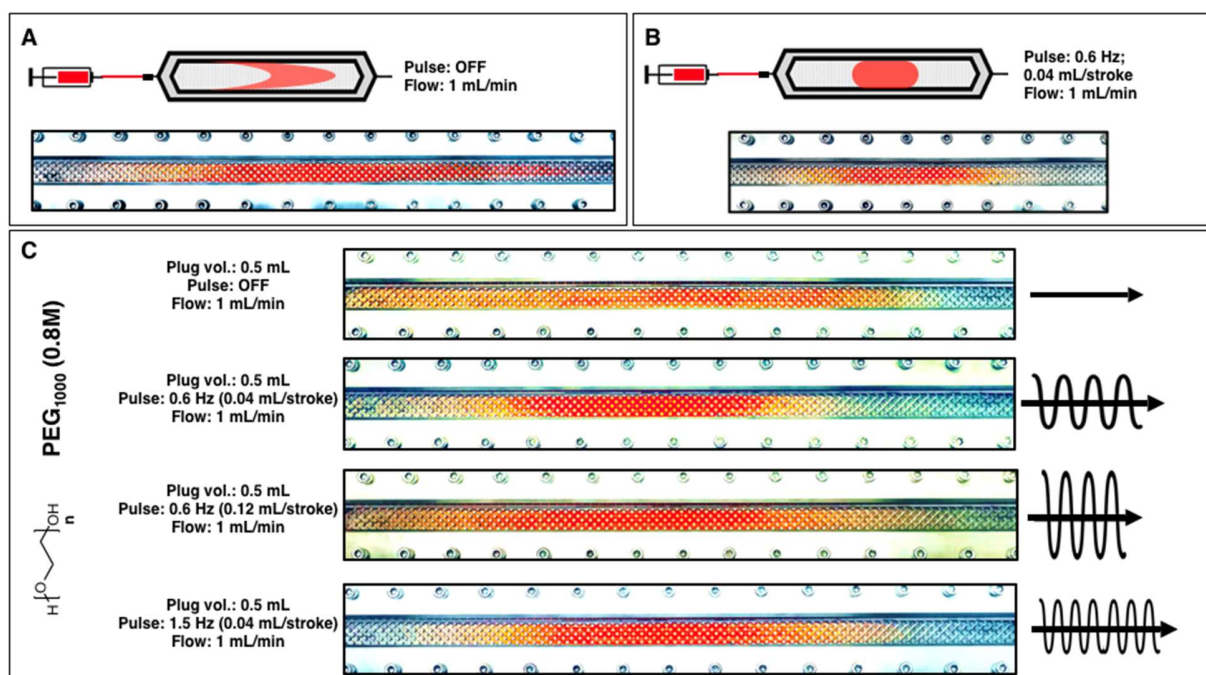


**Figure 1.** Photograph of the flow profile using acetone as a medium. **A)** A crescent-shaped flow profile is visible as a result of the formation of a lateral velocity gradient within the reactor in the absence of pulsation. **B)** A compact flow profile resulting from pulsation leads to a more homogeneous distribution of the medium in both the longitudinal and lateral direction. **C)** A comparison of higher viscosity flow profiles with respect to increasing pulsation frequency and -amplitude.

Typical laminar flow occurs when mixing is limited to diffusion. The combination of static mixers/pillars and pulsation enable rapid mixing in all directions in a relatively short timescale, providing turbulent flow characteristics across a broad range of flow rates. In practice, the turbulent mixing promotes consistent reactions, leading ultimately to polymers with dispersities that are limited by the reaction kinetics, as opposed to being influenced predominantly by mixing profiles. As the pulsation amplitude increases, the longitudinal displacement of the plug per pulse increases and results in the undesirable spread seen in the flow profile analysis (Figure 1C).

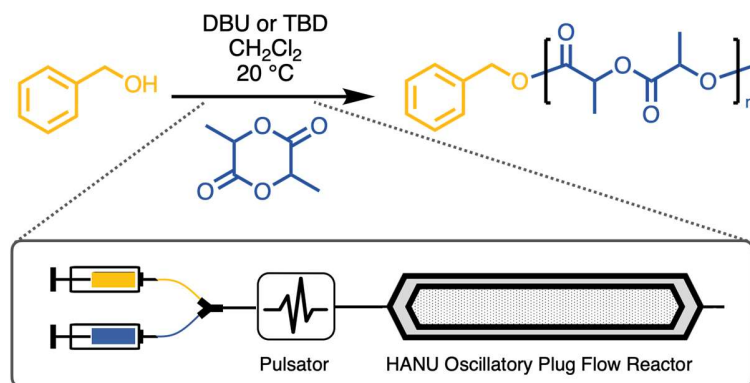
**PLA synthesis using constant monomer to initiator ratio:** PLA has been produced in various continuous-flow reactor setups, including tubular flow and microfluidic devices.<sup>22, 34-37</sup> Several of

these examples employed highly active organocatalysts that afford low dispersity, controlled polymers with astounding efficiency.<sup>49, 50</sup> In particular, we have chosen two common organocatalysts to explore in this investigation, namely 1,8-diazabicyclo[5.4.0]undec-7-ene (DBU) and 1,5,7-triazabicyclo[4.4.0]dec-5-ene (TBD).

Synthesizing amorphous PLA via ROTEP in flow was performed as a means to evaluate various key reactor parameters such as flow rate, pulsation frequency, and -amplitude on molecular attributes (e.g., monomer conversion, molar mass, and dispersity). Initially, homopolymer PLA was synthesized via ROTEP using benzyl alcohol (BA) as an initiator and DBU as a catalyst, maintaining a constant monomer to initiator ratio ([LA]:[BA] = 100) for entries 1–8, while varying the oscillation conditions (Scheme 1; Table 1; Figure S2). Importantly, the LA monomer and initiator were placed in the same syringe before injection, while the catalyst solution was prepared in a separate syringe. This translates to an effect on molecular attributes, owing to different mixing efficiencies (*vide infra*). Conversion was monitored with <sup>1</sup>H NMR spectroscopy of the crude samples (Figure S3). A systematic approach revealed that high conversions (> 80%) were only achieved with flow rates ranging from 0.5 – 2 mL/min, whereas both higher flow rates (5 mL/min) and lower flow rates (0.5 mL/min) resulted in lower conversions (< 60%) at a fixed pulsation setting (0.6 Hz; 0.04 mL/stroke). At fast flow rates, the residence time is too low to allow for sufficient monomer conversion using this particular reactant/catalyst concentrations. Contrarily, at lower flow rates, it is postulated that the effectiveness of the static mixtures are compromised, ultimately resulting in poor mixing between the catalyst and monomer/initiator solutions. This likely results in significantly retarded reaction kinetics compared with moderately faster flow rates. Thus, the optimum flow rate was identified as 1.0 mL/min for exploring additional parameters. The dispersity (Đ) was relatively low (< 1.2) for all samples, with the exception of 0.5 mL/min (entry 1). This further corroborates the hypothesis of poor mixing at very low flow rates, which is ultimately reflected in the moderately higher dispersity. suggesting consistently low RTD, independent of flow rate.



**Scheme 1.** Oscillatory plug flow polymerization of lactide using benzyl alcohol initiator.



Similarly, the effect of pulsation frequency on monomer conversion and dispersity was also investigated. The lowest tested frequency (0.6 Hz) combined with a low amplitude (0.04 mL/stroke) provided the highest conversion along with low dispersity ( $\text{Đ} = 1.15$ ). Notably, in the absence of pulsation, the reaction efficiency drastically declined marginally, while the dispersity was not adversely affected. It is postulated that no pulsation has a minimal effect in these circumstances owing primarily to the fact that the initiator and monomer are already pre-mixed before injection into the reactor. The effect of pulsation becomes much more pronounced in experiments that require mixing of initiator and monomer inside the reactor (vide infra, block polymer synthesis). Otherwise, conversion was only marginally affected by varied pulsation frequency. In contrast, increasing the pulsation amplitude above 0.04 mL/stroke (5%) negatively impacts polymerization efficiency, evident in the lower conversion and lower molar mass indicated by size exclusion chromatography (SEC) (Figure 2, Table 1). Likewise, the dispersity increases very slightly with increased pulsation amplitude (entry 6–8). These results align with the flow profile analysis where a similar trend was observed using a polymer solution with comparable viscosity. Overall, pulsation amplitude contributes more significantly to the product characteristics for the ring-opening polymerization of lactide. Low pulsation amplitude enables efficient mixing

1 without compromising the compact plug flow behavior (i.e., RTD). Notably, in the simple  
2 comparison of ROTEP using related organocatalysts in traditional tubular flow reactors, similar  
3 conversion and dispersities are achieved within the OFR reactor. The real highlight of the OFR in  
4 this context is in scalability. Increasing tube diameter in an effort to accommodate higher flux  
5 leads to lower conversion and broader RTD, reflected by higher dispersities.<sup>47</sup>

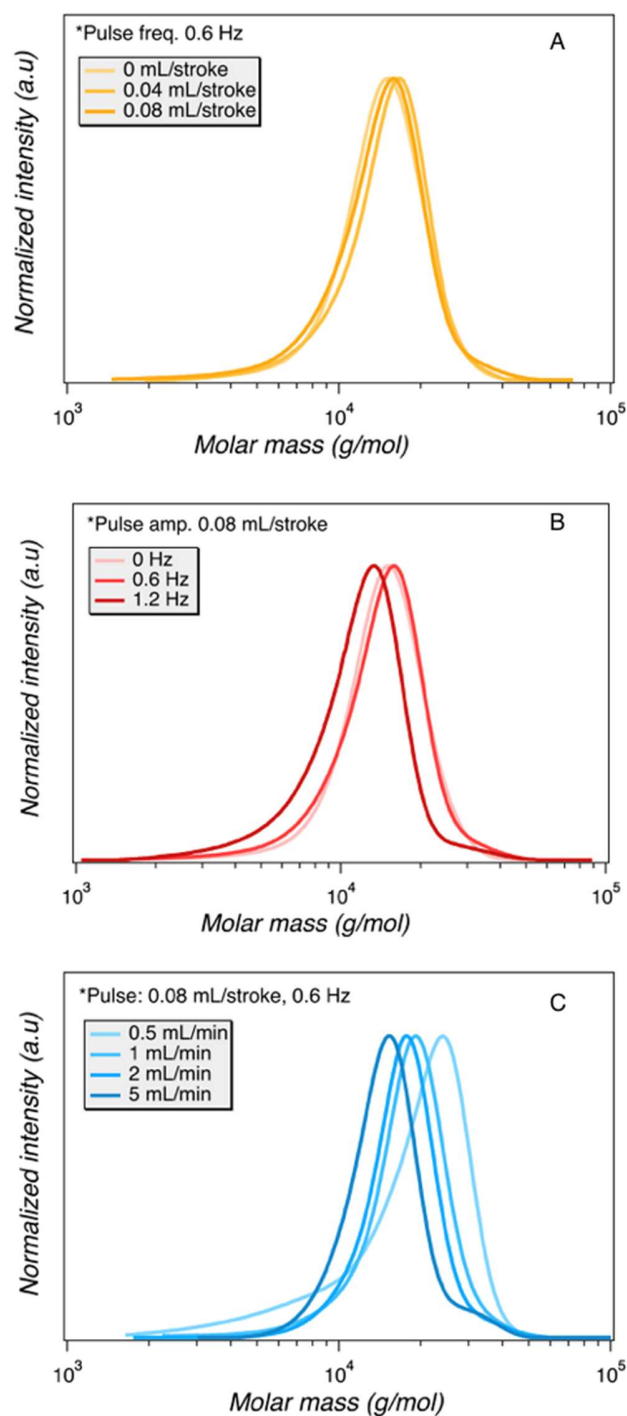


**Figure 2.** Summary SEC chromatograms of different individual parameter variation on molecular weight and distributions. **A)** The effect of pulsation amplitude. **B)** The effect of pulsation frequency. **C)** the effect of flowrate. All polymers had a target molar mass of 14.4 kg/mol.

**Table 1.** Summary of parameter investigation. Selection of the optimal setting is highlighted in green and was based on high conversions (> 90%) with low dispersities (<1.2).

Entry	Flow rate (mL/min)	Amp. (mL/stroke)	Freq. (Hz)	[LA]/[BA]	$M_{n, \text{trgt}}$ (kg/mol) <sup>a</sup>	$M_{n, \text{expt}}$ (kg/mol) <sup>b</sup>	Conv. (%)	$\bar{D}^c$
1	0.5	0.04	0.6	100	14.4	17.5	35	1.39
2	1.0	0.04	0.6	100	14.4	11.4	95	1.16
3	2.0	0.04	0.6	100	14.4	15.7	82	1.11
4	5.0	0.04	0.6	100	14.4	2.4	49	1.12
5	1.0	0	0.0	100	14.4	14.2	79	1.16
6	1.0	0.040.08	0.6	100	14.4	14.4	84	1.15
7	1.0	0.08	0.6	100	14.4	14.2	77	1.20
8	1.0	0.08	1.2	100	14.4	12.2	72	1.22

<sup>a</sup> Target molar masses are calculated from the LA to BA ratios, assuming 100% monomer conversion. <sup>b</sup> Experimental molar masses are determined from end-group analysis using <sup>1</sup>H NMR spectroscopy. <sup>c</sup> Dispersity was determined from SEC in chloroform eluent relative to polystyrene standards.

**Poly(lactide) synthesis using variable monomer to initiator ratio:** The ability to prepare a series of different polymers in a single stream by varying the individual reactant input rates is one of the most appealing advantages of using flow technology. We set out to vary the monomer to initiator ratio ([LA]:[BA]) in situ, which required multiple syringe injection ports that are independently controlled. Aiming for an operationally simple approach, the number of ports was kept at two. The catalyst was therefore included in the initiator solution. This means that changing the relative monomer and initiator feed rates will accompany a change in catalyst concentration. Therefore, the range of catalyst (i.e., DBU) concentrations that were suitable for achieving desired product targets was initially explored. A preliminary experiment was carried out to estimate a rate constant by varying the lactide to DBU catalyst ratio for various plugs. <sup>1</sup>H NMR analysis of monomer conversion revealed a direct relationship with DBU concentrations; more catalyst led to

higher monomer conversion over the same residence time (i.e., flow rate). This data was used to roughly estimate a rate constant (Figure 3, Figure S4, Table 2). In this manner, the rate constant enables us to design a system wherein the flow rates are adjusted *in situ* to reach maximum conversion, taking into account the different target ratios of [LA]:[BA]. The operational conditions are simply tuned to compensate for the variable DBU concentration as the target molar mass is changed, employing the optimal time needed to reach 90% monomer conversion. Importantly, the series of PLA samples was generated in a single experiment, wherein the flow rates of the catalyst solution were merely adjusted relative to monomer flow rates to generate independent plugs corresponding to the indicated [LA] to [DBU] ratios.

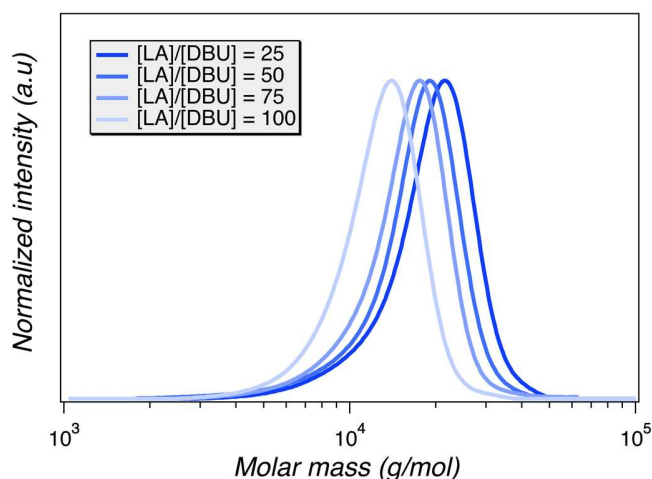


**Figure 3.** SEC chromatograms corresponding to the samples of PLA using various concentrations of DBU catalyst per plug. All samples were generated at fixed flow settings deemed optimal following the flow profile analysis (1 mL/min; 0.6 Hz; 0.04 mL/stroke).

**Table 2.** Data correlating to the DBU reaction kinetics investigation employing a constant RTD via 1 mL/min flow rate, 0.6 Hz frequency, and 0.04 mL/stroke amplitude.

[LA]:[DBU]	Conv. <sup>a</sup> (%)	$M_n^a$ (kg/mol)	$\bar{D}^b$
25	95.3	20.5	1.20
50	94.0	13.5	1.17
75	76.1	14.6	1.14
100	42.5	9.1	1.12

<sup>a</sup> Conversion and experimental molar masses determined from end-group analysis using <sup>1</sup>H NMR spectroscopy. <sup>c</sup> Dispersity was determined from SEC in chloroform eluent relative to polystyrene standards.

This crude kinetic data was used to guide the setup for an experiment in which the target molar mass was adjusted through the LA to BA ratios. One syringe was loaded with LA in CH<sub>2</sub>Cl<sub>2</sub> (1 M) and another smaller syringe was loaded with both initiator (BA) and catalyst (DBU) at a concentration that was determined in order to accommodate a reasonably wide molar mass window without compromising kinetics. However, this design inherently necessitates a change in the overall flow rate to compensate for the lower catalyst concentrations, which is exacerbated in samples with relatively large target molar mass. Decreasing initiator concentration indeed led to an increasing trend in the product molar mass, albeit much less pronounced than expected as indicated by small shifts in the chromatograms (Figure S5, Table S1). In fact, <sup>1</sup>H NMR suggested no increase in molar mass between samples for which the ratio of [LA]:[BA] concentration was increased from 200 to 300. Additionally, the obtained molar mass for all samples as measured by <sup>1</sup>H NMR was significantly lower than the target molar mass suggesting an acute change in catalytic activity with the different concentrations. Lower concentrations of DBU may lead to retarded reaction kinetics that were not apparent in the initial investigation of a systematic DBU decrease. Operational simplicity is an important factor moving forward, wherein the number of

injection ports was strictly limited to two. A critical design criterium is that the initiator and catalyst should be combined in one syringe. In order to access the broadest array of polymer makeup through adjusting the individual feed rates, the catalyst activity should be as high as possible. This decouples the relative feed rates from the final LA monomer conversion. For this reason, 1,5,7-triazabicyclo[4.4.0]dec-5-ene (TBD) was investigated in further experiments due to its strong basic properties and high reactivity.<sup>49</sup>

**LFL triblock copolymer synthesis in flow:** In a further extension of this methodology, telechelic poly( $\beta$ -farnesene)-diol (PFD) was used as a macroinitiator to generate ABA-type triblock copolymers from the ROTEP of LA. The commercial PFD was provided by Cray Valley (tradename KRASOL F3000) with a molar mass of 2.8 kg/mol verified by <sup>1</sup>H NMR spectroscopy using end-group analysis (Figure S6). Performing the ROTEP using the telechelic PFD ideally leads to symmetric triblock copolymers with final compositions targeted by adjusting the flow rates of PFD relative to LA using two independent syringe feeds. Feed ratios are adjusted by taking into account the anticipated LA monomer conversion. Triblocks are labeled as LFL (X:Y), where X and Y are the relative mass ratios of LA and PFD in the feed, respectively.

The reaction setup using PFD was analogous to the previously described experimental protocol using benzyl alcohol, but employing a more active catalyst, TBD (Figure 4). Initially a 1:1 weight ratio of PLA to PFD was targeted to generate LFL (1:1). A comparison was initially made between DBU and TBD catalysts using various flowrates, unambiguously revealing that TBD resulted in higher conversions across a range of residence times (Figure S7). Nearly complete polymerization was even achieved at 5 mL/min flow rate with TBD, generating polymers with relatively low dispersities. This flow rate translates to >80 g/h of symmetric triblock polymers at a LA concentration of 1 M. Optimized experimental conditions resulted in consistently low dispersities ( $\bar{M}_w/\bar{M}_n \sim 1.3$ ) and relatively high conversion (> 90%) for all evaluated flow rates (Table S2). <sup>1</sup>H NMR analysis of the samples using TBD in CHCl<sub>3</sub> suggested that the product molar mass

was consistent across the range of residence times investigated and experimental values were in good agreement with the target  $M_n$  of 5.6 kg/mol (Figure S7; Table S2). Additionally, the  $^1\text{H}$  NMR spectra of the ABA block copolymers suggest that initiation was essentially quantitative from the poly(farnesene)-diol owing to the transition of characteristic end-group signals as the hydroxyl groups are transformed to esters (Figure 5A).

The block architecture was further corroborated with differential scanning calorimetry (DSC). Characteristic glass transition temperatures ( $T_g$ ) corresponding to both the PFD and PLA blocks can be observed in the block copolymer product, suggesting successful incorporation of the PLA substituents onto the poly(farnesene)-diol macroinitiator (Figure 5B). The  $T_g$  corresponding to the PLA blocks is significantly depressed compared with PLA homopolymer. This is consistent with the relatively low molar mass of the PLA blocks and the tethered architecture in the ABA block copolymer, restricting segmental motion.<sup>51</sup>

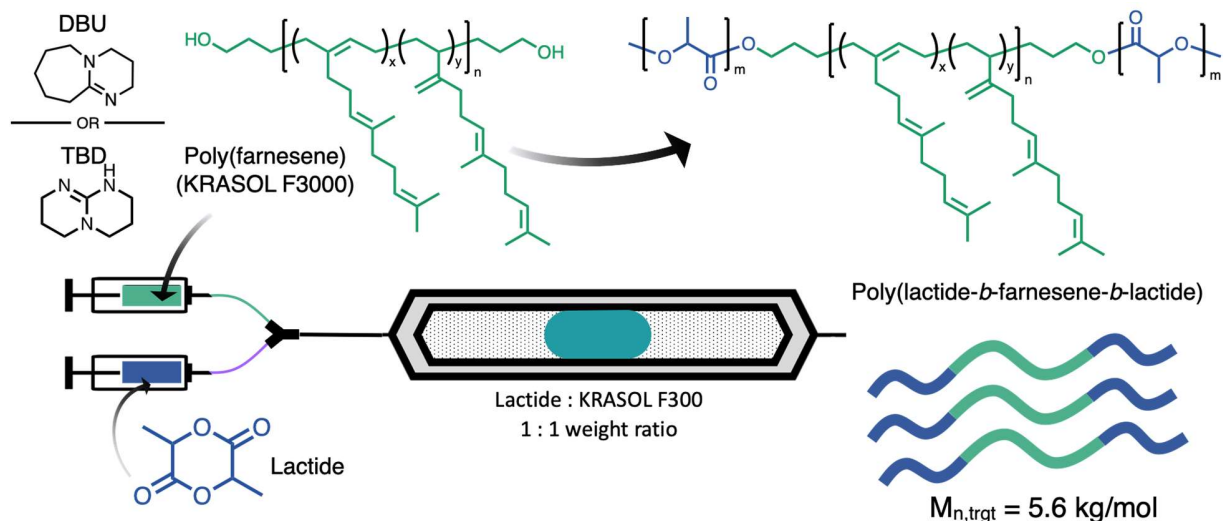


**Figure 4.** Schematic overview of LFL triblock polymer synthesis using the HANU flow reactor.



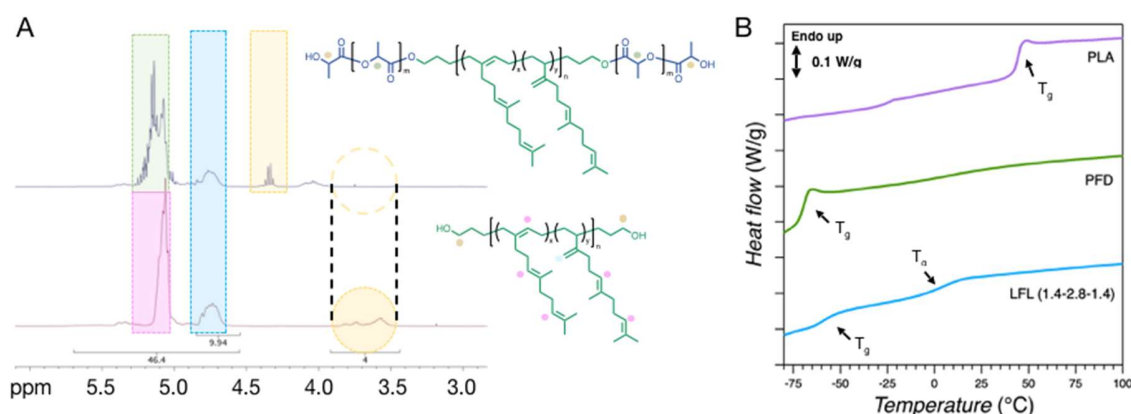


**Figure 5.** (A) <sup>1</sup>H NMR analysis comparing commercial PFD and the LFL triblock copolymer. (B) DSC analysis of the synthesized LFL triblock copolymer, as well as PLA and the commercial PFD. Characteristic *T<sub>g</sub>*s are labelled for each sample.

**LFL series synthesis in flow:** Varying the target composition of the symmetric LFL triblock copolymers *in situ* was performed similarly to the analogous experiment using benzyl alcohol. However, because the more active TBD catalyst has been employed, the residence time/flow rate compensation is unnecessary with changing monomer concentration. This was because previous results suggest the polymerization reaction was nearly complete in all cases, irrespective of residence time. High conversion ( $\geq 94\%$ ) was achieved for all target compositions of PLA according to <sup>1</sup>H NMR spectroscopy and molar masses ( $M_n$ ) were in good agreement with theoretical values (Table 3). This was confirmed using <sup>1</sup>H NMR analysis showing a gradual increase in corresponding PLA peak intensity (Figure S8), as well as SEC, where increased molar mass relative to PFD precursor is apparent as the concentration of LA per plug was increased (Figure 6A). Surprisingly, the dispersity increased moderately with each consecutive sample, reaching a value of  $\bar{D} = 1.5$  for the last two compositions. The origin of this unexpected result was investigated by performing the experiment again, starting with the highest wt:wt ratio, targeting LFL (4:1). This composition was targeted in four sequentially prepared samples, with increasing pulsation frequencies (0.6 Hz, 1.2 Hz, 1.8 Hz, and 2.4 Hz). The results suggest optimal conversion was achieved for all pulsations whilst the dispersity remained relatively constant and was

generally in agreement with the previous experiment (Figure S9, Table S3). These results suggest that the previously observed moderately high dispersity with higher molar masses is not related to the higher lactide concentration in itself, nor is it attributed to different pulsation frequencies. Rather, it is posited that this is an artifact of residual reagents from consecutive plugs. A small volume (< 0.5 mL) of each plug inadvertently remains in a small section of tubing in syringe injection port and the T-crossing connected to the HPLC pump. As the ratio of PFD to LA varies across sequential plugs, any residual reagents of a different concentration ratio will contribute to the subsequent sample and thus increase the dispersity. This problem will be overcome in future investigations by briefly flushing the tubing with the desired reagent ratio prior to loading the plug.

**Table 3.** Analysis of poly(lactide-*b*-farnesene-*b*-lactide) block copolymer synthesis in flow via *in situ* tuning of wt:wt ratios of lactide to poly(farnesene)-diol. All experiments were performed at 2 mL/min using 0.04 mL/stroke pulsation at 0.6 Hz.

[LA]:[PFD] (wt:wt)	[LA]:[TBD] (mol:mol)	$M_n$ (theo) (kg/mol)	Conv. (%)	$M_n$ (NMR) (kg/mol)	$M_n$ (SEC) (kg/mol)	$\phi_L$	$\bar{D}$
1:1	57	5.6	94	5.1	6.8	0.45	1.24
2:1	114	8.6	95	8.1	9.6	0.65	1.34
3:1	170	11.5	98	10.1	11.5	0.72	1.51
4:1	225	14.4	96	14.9	15.2	0.81	1.51

*Complementary block polymer synthesis targeting identical compositions was performed in the OFR in the absence of any pulsation. Chromatograms from SEC analysis have markedly different distributions (Figure S10; Table S4). The associated dispersities for all samples are significantly larger, consistent with poor mixing. This is in contrast to the results from homopolymer synthesis, wherein the dispersity was not substantially influenced by pulsation. The block polymer synthetic protocol differs in a critical aspect, with the (macro)initiator and the LA monomer being*

injected from different syringes. This setup is necessary to enable the streamlined synthesis of a library of compositionally variable samples in a single experiment. However, the independent injection of initiator and monomer also requires intimate mixing to occur immediately upon injection, which is made more challenging with higher viscosity macroinitiator solution of PFD. Thus, the pulsation provides an essential mixing of the reactants in order to achieve uniform polymerization conditions (i.e., low dispersity), which was unnecessary during the synthesis of PLA homopolymer.

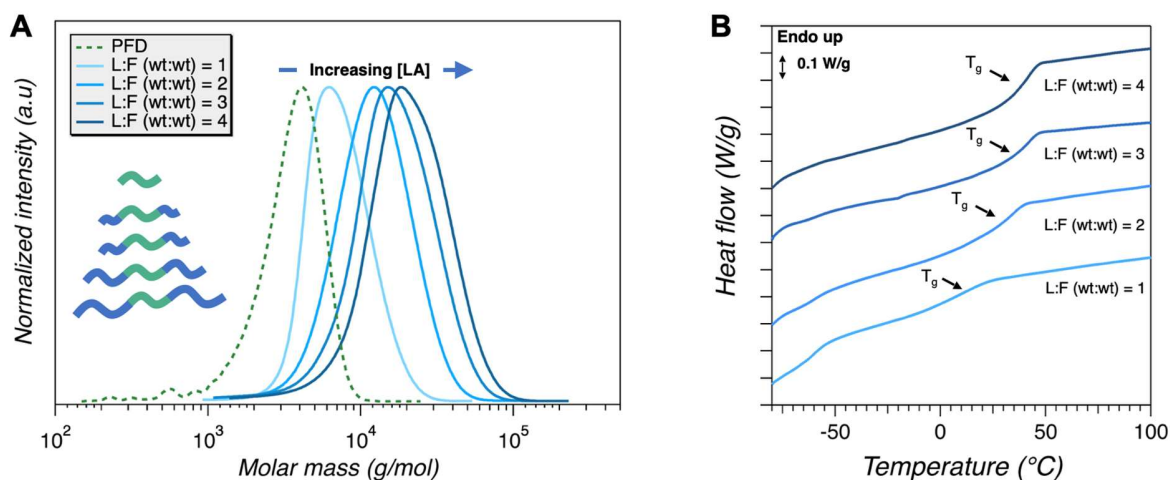


**Figure 6.** (A) SEC analysis and (B) DSC thermograms of LFL triblock copolymers with various compositions.

Finally, DSC was performed on the different triblock copolymers (Figure 6B). An unambiguous increase of the  $T_g$  of the PLA component is observed as L:F (wt:wt) increases (i.e., increasing PLA content). As the length of the PLA chain increases in the LFL triblock copolymer, the free volume of the end groups will increase, thereby inducing a higher  $T_g$  as described by the Flory – Fox equation.<sup>51</sup> These data are consistent with the different compositions indicated by molecular analysis and the correspondingly varying molar mass of the PLA blocks.

## CONCLUSION

An oscillatory flow reactor (i.e., HANU flow reactor) was used to perform continuous polymerization reactions for the first time. Through initial dye tracer experiments, visual observations were conducted to evaluate the effect of flow pulsation on the flow profile behavior. The obtained data revealed that the implementation of an oscillatory flow in constrained process channel dimensions can have a considerable effect on the polymer product outcome. These first observation will be critical to further assess polymerization studies carried out using this novel flow reactor type system. Providing an overview of the crucial process parameters and the possibility to obtain on-demand control over your polymerization characteristics highlight the added value of continuous polymerization in OFRs. Additionally, we were able to verify the flow profile analysis using the ring opening transesterification polymerization (ROTEP) of D,L-lactide. Follow-up experiments indicated that, when optimized with an efficient organocatalyst, targeted molar masses of ABA-type poly(lactide-*b*-farnesene-*b*-lactide) triblock copolymers could be synthesized at relatively high flow rates and high conversions via *in situ* modulation of the reagent concentrations. A change in various molecular properties was then confirmed using a variety of analytical techniques demonstrating the efficiency and tuneability with which the HANU flow reactor can be utilized to achieve specific polymer architectures for various commercial purposes. We believe that this study has provided the foundation for future polymer research using OFRs in order to realize polymer architectures of increasing complexity with uncompromised efficiency, accuracy, and eventual scalability. Some critical challenges that remain include ensuring more controlled molecular attributes by systematic adjustment of process parameters, reflected foremost in low dispersity. Further, pushing the boundaries toward high molar mass materials, with correspondingly high viscosity remains. A lastly, maintaining the control over molecular attributes while pushing toward high throughput will be a challenge, keeping a keen eye on scale-up.

## AUTHOR CONTRIBUTIONS

L.M.P, M.D.H and H.G. helped design the experimental approach and aided with data interpretation. M.D.H conducted all of the experiments. All authors contributed to writing and editing the manuscript.

## CONFLICTS OF INTEREST

There are no conflicts to declare.

## ACKNOWLEDGMENTS

We greatly appreciate the generous support of Creaflow B.V. for contributing the reactor equipment (i.e. HANU flow reactor), which was utilized to accommodate the polymerization reactions in light of this project. Partial financial support from Hasselt University under the project Bijzonder Onderzoeksfond (BOF) R-12788 (BOF22K04) is also greatly appreciated.

**ELECTRONIC SUPPLEMENTARY INFORMATION (ESI) available:** Materials and methods, experimental procedures, and additional characterization data.

## REFERENCES

1. H. B. Feng, X. Y. Lu, W. Y. Wang, N. G. Kang and J. W. Mays, *Polymers*, 2017, **9**.
2. F. S. Bates and G. H. Fredrickson, *Annu. Rev. Phys. Chem.*, 1990, **41**, 525-557.
3. M. W. Matsen and F. S. Bates, *J. Chem. Phys.*, 1997, **106**, 2436-2448.
4. G. P. Baeza, *J. Polym. Sci.*, 2021, **59**, 2405-2433.
5. A. Phatak, L. S. Lim, C. K. Reaves and F. S. Bates, *Macromolecules*, 2006, **39**, 6221-6228.
6. G. Fleury and F. S. Bates, *Macromolecules*, 2009, **42**, 3598-3610.
7. F. S. Bates, M. A. Hillmyer, T. P. Lodge, C. M. Bates, K. T. Delaney and G. H. Fredrickson, *Science*, 2012, **336**, 434-440.
8. J. Y. Zhang, D. K. Schneiderrnan, T. Q. Li, M. A. Hillmyer and F. S. Bates, *Macromolecules*, 2016, **49**, 9108-9118.
9. Z. L. Li, M. Tang, S. Liang, M. Y. Zhang, G. M. Biesold, Y. J. He, S. M. Hao, W. Choi, Y. J. Liu, J. Peng and Z. Q. Lin, *Prog. Polym. Sci.*, 2021, **116**.
10. L. M. Pitet, B. M. Chamberlain, A. W. Hauser and M. A. Hillmyer, *Macromolecules*, 2010, **43**, 8018-8025.
11. J. Bolton and J. Rzaev, *ACS Macro Lett.*, 2012, **1**, 15-18.
12. M. K. Mahanthappa, F. S. Bates and M. A. Hillmyer, *Macromolecules*, 2005, **38**, 7890-7894.

- 1 13. N. Zaquen, M. Rubens, N. Corrigan, J. T. Xu, P. B. Zetterlund, C. Boyer and T. Junkers,  
2 *Prog. Polym. Sci.*, 2020, **107**.
- 3 14. M. H. Reis, F. A. Leibfarth and L. M. Pitet, *ACS Macro Lett.*, 2020, **9**, 123-133.
- 4 15. A. Nagaki, A. Miyazaki and J. Yoshida, *Macromolecules*, 2010, **43**, 8424-8429.
- 5 16. J. Vandenberg, T. d. m. Ogawa and T. Junkers, *J. Polym. Sci., Part A: Polym. Chem.*,  
6 2013, **51**, 2366-2374.
- 7 17. A. Nagaki, K. Akahori, Y. Takahashi and J. Yoshida, *J. Flow Chem.*, 2014, **4**, 168-172.
- 8 18. J. Vandenberg, T. Tura, E. Baeten and T. Junkers, *J. Polym. Sci., Part A: Polym. Chem.*,  
9 2014, **52**, 1263-1274.
- 10 19. B. Wenn, M. Conradi, A. D. Carreiras, D. M. Haddleton and T. Junkers, *Polym. Chem.*,  
11 2014, **5**, 3053-3060.
- 12 20. M. Chen and J. A. Johnson, *Chem. Commun.*, 2015, **51**, 6742-6745.
- 13 21. N. Corrigan, D. Rosli, J. W. J. Jones, J. T. Xu and C. Boyer, *Macromolecules*, 2016, **49**,  
14 6779-6789.
- 15 22. W. J. Huang, N. Zhu, Y. H. Liu, J. Wang, J. Zhong, Q. Sun, T. Sun, X. Hu, Z. Fang and K.  
16 Guo, *Chem. Eng. J.*, 2019, **356**, 592-597.
- 17 23. N. Zaquen, A. Kadir, A. Iasa, N. Corrigan, T. Junkers, P. B. Zetterlund and C. Boyer,  
18 *Macromolecules*, 2019, **52**, 1609-1619.
- 19 24. M. Rubens, J. H. Vrijssen, J. Laun and T. Junkers, *Angew. Chem. Int. Ed.*, 2019, **58**, 3183-  
20 3187.
- 21 25. C. P. Breen, A. M. K. Nambiar, T. F. Jamison and K. F. Jensen, *Trends in Chemistry*, 2021,  
22 **3**, 373-386.
- 23 26. M. Reis, F. Gusev, N. G. Taylor, S. H. Chung, M. D. Verber, Y. Z. Lee, O. Isayev and F.  
24 A. Leibfarth, *J. Am. Chem. Soc.*, 2021, **143**, 17677-17689.
- 25 27. C. Tonhauser, A. Natalello, H. Löwe and H. Frey, *Macromolecules*, 2012, **45**, 9551-9570.
- 26 28. Y. H. Su, Y. Song and L. Xiang, *Top. Curr. Chem.*, 2018, **376**, 44.
- 27 29. W. Debrouwer, W. Kimpe, R. Dangreau, K. Huvaere, H. P. L. Gemoets, M. Mottaghi, S.  
28 Kuhn and K. Van Aken, *Org. Process Res. Dev.*, 2020, **24**, 2319-2325.
- 29 30. C. Rosso, S. Gisbertz, J. D. Williams, H. P. L. Gemoets, W. Debrouwer, B. Pieber and C.  
30 O. Kappe, *React. Chem. Eng.*, 2020, **5**, 597-604.
- 31 31. M. Wernik, G. Sipos, B. Buchholz, F. Darvas, Z. Novak, S. B. Otvos and C. O. Kappe,  
32 *Green Chem.*, 2021, **23**, 5625-5632.
- 33 32. P. Bianchi, J. D. Williams and C. O. Kappe, *Green Chem.*, 2021, **23**, 2685-2693.
- 34 33. J. R. McDonough, S. Murta, R. Law and A. P. Harvey, *Chem. Eng. J.*, 2019, **358**, 643-657.
- 35 34. N. Zhu, W. Y. Feng, X. Hu, Z. L. Zhang, Z. Fang, K. Zhang, Z. J. Li and K. Guo, *Polymer*,  
36 2016, **84**, 391-397.
- 37 35. X. Hu, N. Zhu, Z. Fang and K. Guo, *React. Chem. Eng.*, 2017, **2**, 20-26.
- 38 36. W. Adhami, Y. Bakkour and C. Rolando, *Polymer*, 2021, **230**.
- 39 37. C. Bakkali-Hassani, J. P. Hooker, P. J. Voort, M. Rubens, N. R. Cameron and T. Junkers,  
40 *Polym. Chem.*, 2022, **13**, 1387-1393.
- 41 38. F. Della Monica and A. W. Kleij, *Polym. Chem.*, 2020, **11**, 5109-5127.
- 42 39. G. John, S. Nagarajan, P. K. Vemula, J. R. Silverman and C. K. S. Pillai, *Prog. Polym. Sci.*,  
43 2019, **92**, 158-209.
- 44 40. C. Wahlen and H. Frey, *Macromolecules*, 2021, **54**, 7323-7336.
- 45 41. P. A. Wilbon, F. Chu and C. Tang, *Macromol. Rapid Commun.*, 2013, **34**, 8-37.
- 46 42. J. Zhang, J. Chen, M. Yao, Z. Jiang and Y. Ma, *J. Appl. Polym. Sci.*, 2019, **136**, 47673.

1 43. C. Zhou, Z. Wei, X. Lei and Y. Li, *RSC Advances*, 2016, **6**, 63508-63514.  
2 44. Z. K. Wang, L. Yuan and C. B. Tang, *Acc. Chem. Res.*, 2017, **50**, 1762-1773.  
3 45. D. K. Schneiderman and M. A. Hillmyer, *Macromolecules*, 2017, **50**, 3733-3750.  
4 46. Z. R. Zhong, Y. N. Chen, Y. Zhou and M. Chen, *Chin. J. Polym. Sci.*, 2021, **39**, 1069-1083.  
5 47. M. H. Reis, T. P. Varner and F. A. Leibfarth, *Macromolecules*, 2019, **52**, 3551-3557.  
6 48. Y. Zhou, Y. Gu, K. M. Jiang and M. Chen, *Macromolecules*, 2019, **52**, 5611-5617.  
7 49. B. G. G. Lohmeijer, R. C. Pratt, F. Leibfarth, J. W. Logan, D. A. Long, A. P. Dove, F.  
8 Nederberg, J. Choi, C. Wade, R. M. Waymouth and J. L. Hedrick, *Macromolecules*, 2006,  
9 **39**, 8574-8583.  
10 50. A. P. Dove, *ACS Macro Lett.*, 2012, **1**, 1409-1412.  
11 51. M. T. Martello and M. A. Hillmyer, *Macromolecules*, 2011, **44**, 8537-8545.  
12  
13  
14

For Table of Contents

# Fully Biobased Triblock Copolymers Generated Using An Unconventional Oscillatory Plug Flow Reactor

Milan Den Haese, Hannes Gemoets, Koen Van Aken, Louis M. Pitet<sup>†</sup>

